Wiley
Computational and Mathematical Methods
Volume 2024, Article ID 5589805, 12 pages
https://doi.org/10.1155/2024/5589805

WILEY

*Research Article*

# A Mathematical Analysis of the Impact of Immature Mosquitoes on the Transmission Dynamics of Malaria

**Nantogmah Abdulai Sualey**[1], **Philip N. A. Akuka**[2], **Baba Seidu**[1] and **Joshua Kiddy K. Asamoah**[3,4]

[1]*Department of Mathematics, School of Mathematical Sciences, C. K. Tedam University of Technology and Applied Sciences, Navrongo, Ghana UK-0215-5321*
[2]*Department of Mathematics, Bongo Senior High School, Bongo, Ghana*
[3]*Department of Mathematics, Saveetha School of Engineering SIMATS, Chennai, India*
[4]*Department of Mathematics, Kwame Nkrumah University of Science and Technology, Kumasi, Ghana*

Correspondence should be addressed to Baba Seidu; bseidu@cktutas.edu.gh

Received 5 April 2024; Revised 30 August 2024; Accepted 17 September 2024

Academic Editor: Yunfeng Wu



This study delves into the often-overlooked impact of immature mosquitoes on the dynamics of malaria transmission. By employing a mathematical model, we explore how these aquatic stages of the vector shape the spread of the disease. Our analytical findings are corroborated through numerical simulations conducted using the Runge–Kutta fourth-order method in MATLAB. Our research highlights a critical factor in malaria epidemiology: the basic reproduction number ($\mathcal{R}_0$). We demonstrate that when $\mathcal{R}_0$ is below unity ($\mathcal{R}_0 < 1$), the disease-free equilibrium exhibits local asymptotic stability. Conversely, when $\mathcal{R}_0$ surpasses unity ($\mathcal{R}_0 > 1$), the disease-free equilibrium becomes unstable, potentially resulting in sustained malaria transmission. Furthermore, our analysis covers equilibrium points, stability assessments, bifurcation phenomena, and sensitivity analyses. These insights shed light on essential aspects of malaria control strategies, offering valuable guidance for effective intervention measures.

**Keywords:** basic reproduction number; bifurcation; Runge–Kutta fourth-order method; sensitivity; stability

## 1. Introduction

*Plasmodium* is the parasite that causes malaria, which is a protozoan disease. The female Anopheles mosquito, which has an estimated lifespan of at least 5 months, is the carrier of this parasite. The typical lifespan of their male counterparts is barely 6–7 days. The *Plasmodium* parasite causing malaria in humans is typically divided into four kinds. We have the vivax, falciparum, malariae, and ovale. Ninety-five percent of incidences come from the first two [1]. Malaria is usually transmitted after a female Anopheles mosquito carrying the parasite stings a victim. High fever, headache, sweating, chills, and shivering with a drop in body temperature are all signs of malaria. In severe cases, there is anaemia, enlarged liver and spleen, and general ill health. Malaria has been globally considered a problem. The World Health Organization approximated that about 178 million infections were confirmed [2]. Out of this, African countries contributed 171 million, and Ghana, almost 7 million cases. An attempt to control and eliminate pathogens responsible for the spread of communicable diseases has been of great interest in the field of public health as far back as the early 1950s. In the 1960s, there were indications of hope from the practices that seemed to eliminate these diseases. Improved sanitation and the use of antibiotics were contributing factors to the elimination of most infectious diseases. Nonetheless, these agents, with time, get adapted to the control strategies and resurface in probably different forms [3]. Organisms' medical resistance resulting in the growth of new forms of microorganisms and diseases is usually related

to population growth, climate change, increased urbanization, and increased travel. A lot of research has been conducted employing mathematical modelling to understand the dynamics of diseases and strategies for combatting them [4–10]. Malaria has been a menace and sometimes fatal epidemic disease that affects about half or a greater portion of the world's populace. The World Health Organization estimated a total of 168 million confirmed cases of malaria were recorded in 2016, which rose to 241 million cases in 2020 [2]. Whitty and Ansah [11] estimated that the number of deaths resulting from malaria stood at 435,000 in 2019. Malaria stands fifth in the world in terms of infectious diseases leading to death while being second in Africa. Due to this, a number of research has been made by a whole lot of researchers interested in the eradication of the disease. Oke et al. [12] formulated a mathematical model for malaria, taking into consideration control measures such as treated bed nets, medication, and insecticide spray. Their study revealed that the combination of treatment and treated bed nets is the best control measure. Further, Abioye et al. [13] proposed a malaria model incorporating four control strategies: insecticide-treated bed net control, infected human treatment control, sterile mosquito technique control, and use of control on pregnant women and newborn births. They concluded that if the controls are well managed and implemented, then it would curb or limit the transmission of malaria between vector–host–related populations. Iboi, Gumel, and Taylor [14] presented a new mathematical model for assessing the impact of sterile insect technology (SIT) and seasonal variation in local temperature on the population abundance of malaria mosquitoes in an endemic setting. These research works were based on adult mosquitoes.

In a study of Layie et al. [15], an agent-based model (ABM) was proposed to assess and examine the impact of mosquito's aquatic habitat (AH) destruction program and also bring out guidelines for larval source management (LSM) by AH destruction. They also took into account the questing–resting to represent the number of infectious bites in our ABM which had not yet been carried out until now. Also, Koutou, Traoré, and Sangaré [16] proposed the vector population dynamic model including autoregulation phenomena of eggs, larvae, and pupae. Their results showed that the effect of immature stages is very important in the mosquito's population proliferation. Traoré, Koutou, and Sangaré [17] formulated a deterministic mathematical model of malaria transmission by incorporating seasonality. They took into account the four distinct mosquito metamorphic stages. It was coupled with two submodels, namely, the model of mosquito population and the model of malaria parasite transmission due to the interaction between mosquitoes and humans. Very few work has been done considering the immature stages (egg, larva, and pupa) of the vector as cited above, yet these stages of mosquitoes play a major role in the transmission of malaria. They grow into infected adult mosquitoes, and the spread of the disease continues when they could have been economically controlled. Olaniyi et al. [18] presented a model to control malaria transmission dynamics while considering the social classes of the human population and their interaction with the mosquito population. They further classified each social class into three compartments. That is, susceptible, infectious, and recovered with temporal immunity. They also divided the vector population into susceptible and infectious. Their model could not account for the impact of immature mosquitoes on the transmission dynamics and control. Also, Tchoumi et al. [19] proposed a malaria model with an age structure consisting of SEIS for individuals below the age of 5 years and then SEIRS for those aged 6 years and above. The vector population was also put under three compartments, that is, susceptible, exposed, and infectious. The principal objective of their study was to verify if it was justifiable to place emphasis on fighting malaria in children below the age of 5 and also to determine if the preventive measures taken affect the general endemicity of the disease in the human population positively. Their results showed that controlling malaria in children below the age of 5 years when stepped up could eradicate the disease completely. The works of Tchoumi et al. [19] coupled with that of Olaniyi et al. [18] serve as motivation to restructure the human population by adding the vaccinated class to the human population and also the immature stages of the vector to improve the understanding of the transmission dynamics and control of malaria.

This research therefore seeks to present a mathematical epidemiological model that will help investigate the impacts of immature mosquitoes and vaccination on the transmission dynamics of malaria. The paper is divided into the following sections: Section 2 entails the formulated proposed model, while analytical analysis is presented in Section 3. Numerical simulations performed in support of previous sections are captured in Section 4. Finally, Section 5 consists the conclusion.

## 2. Model Formulation

The life cycle of the vector (female Anopheles) passes through four different developmental stages. These include the egg, larval, pupal, and adult stages. The first three stages are considered immature and usually aquatic, while the last stage is arboreal [20, 21]. Blood is sucked when an infected adult female mosquito bites a human. These female mosquitoes feed on the blood of the exposed human, which is then utilized to produce eggs. When conditions are favorable, the eggs that are laid on the surfaces of water hatch into larvae a few days afterwards. In unfavourable conditions such as drought, the eggs may take several months to hatch. The larvae are very small in size. They usually depend on organic matter and algae for food [22, 23]. Larvae are considered cannibal because, under adverse conditions, they feed on earlier-stage larvae. After the larvae have undergone complete moulting, they become pupae. The pupal stage is regarded as the resting and dormant developmental phase. This is a period when the pupae grow into the adult-stage mosquito. Here, the skin of the pupa sheds, and the adult mosquito develops [24, 25]. Therefore, in the model, the mosquito population is divided into two stages, immature and mature stages. The immature compartments at any

given time $(t)$ are further divided into eggs $(E)$, larvae $(L)$, and pupae $(P)$, while the adult $(A)$ mosquito is subdivided into two groups: susceptible mosquitoes $(S_v)$ and infectious mosquitoes $(I_v)$. The total adult vector population is given by $N_v(t) = S_v(t) + I_v(t)$.

Further, individuals in the human population are divided into two groups according to their ages, that is, children (individuals under the age of 5) and adults (individuals above the age of 5). The Children compartment is subdivided into three compartments, namely, susceptible children $(S_c)$, vaccinated children $(V_c)$, and infected children $(I_c)$. Also, the adult humans are categorized as susceptible adults $(S_a)$, infected adults $(I_a)$, vaccinated adults $(V_a)$, and recovered adults $(R_a)$. The total human population is given by

$$N_h(t) = S_c(t) + V_c(t) + I_c(t) + S_a(t) + I_a(t) + R_a(t) + V_a(t)$$

Mosquito eggs hatch and develop into larvae at rate $\alpha_{el}$ and from larvae to pupae and pupae to adult mosquitoes at rates $\alpha_{lp}$ and $\alpha_{pa}$, respectively. Further, mosquito eggs fail to hatch at rate $\mu_e$, and larvae fail to develop into pupae and pupae into adult mosquitoes at rates $\mu_l$ and $\mu_p$, respectively. We consider that all recruits of vectors, children, and adults are put in the susceptible compartments $S_v$, $S_c$, and $S_a$ with constant rates $\Lambda_v$, $\Lambda_c$, and $\Lambda_a$, respectively. Adult mosquitoes, children, and adult humans contract the disease as a result of effective contact with infected female mosquitoes at transmission probabilities of $\lambda_{hv}$, $\lambda_{vc}$, and $\lambda_{va}$, respectively. Malaria transmission is thought to be reduced by vaccination of susceptible children at rate $\nu$. A successful treatment at rates $\rho_c$ and $\rho_a$ of infected children and adults are assumed, while malaria-induced death rates of children and adults are given as $\mu_{cm}$ and $\mu_{am}$, respectively. Natural death rates of human and adult vectors are given as $\mu_h$ and $\mu_v$, respectively. The dynamics stated are pictorially illustrated in Figure 1 and mathematically shown in Equation (1). The various parameters of the model are thus defined in Table 1.

$$\begin{aligned}
&\overbrace{\begin{aligned}
\frac{dE}{dt} &= bN_v - (\alpha_{el} + \mu_e)E,\\
\frac{dL}{dt} &= \alpha_{el}E - (\alpha_{lp} + \mu_l)L,\\
\frac{dP}{dt} &= \alpha_{lp}L - (\alpha_{pa} + \mu_p)P,\\
\frac{dS_v}{dt} &= \Lambda_v + \alpha_{pa}P - (\lambda_{hv} + \mu_v)S_v,\\
\frac{dI_v}{dt} &= \lambda_{hv}S_v - \mu_v I_v,
\end{aligned}}^{\text{Vector Population}}\\
&\overbrace{\begin{aligned}
\frac{dS_c}{dt} &= \Lambda_c + \rho_c I_c - (\mu_h + \nu + \lambda_{vc} + \gamma_2)S_c,\\
\frac{dV_c}{dt} &= \nu S_c - (\mu_h + \gamma_1)V_c,\\
\frac{dI_c}{dt} &= \lambda_{vc}S_c - (\mu_h + \mu_{cm} + \rho_c)I_c,\\
\frac{dS_a}{dt} &= \Lambda_a + \gamma_2 S_c + \ell R_a - (\mu_h + \lambda_{va})S_a,\\
\frac{dI_a}{dt} &= \lambda_{va}S_a - (\mu_h + \mu_{am} + \rho_a)I_a,\\
\frac{dR_a}{dt} &= \rho_a I_a - (\mu_h + \ell)R_a,\\
\frac{dV_a}{dt} &= \gamma_1 V_c - \mu_h V_a,
\end{aligned}}^{\text{Human Population}}
\end{aligned} \tag{1}$$

with nonnegative initial conditions

$$S_c \geq 0, V_c \geq 0, I_c \geq 0, S_a > 0, I_a \geq 0, R_a \geq 0$$
$$V_a \geq 0, E \geq 0, L \geq 0, P \geq 0, S_v \geq 0, I_v \geq 0$$

For convenience, we make the following substitutions:

$$k_1 = \alpha_{el} + \mu_e, k_2 = \alpha_{lp} + \mu_l, k_3 = \alpha_{pa} + \mu_p, k_4 = \mu_h + \nu + \gamma_2$$
$$k_5 = \mu_h + \gamma_1, k_6 = \mu_h + \mu_{cm} + \rho_c, k_7 = \mu_h + \mu_{am} + \rho_a, k_8 = \mu_h + \ell$$

## 3. Basic Properties of the Model

### 3.1. Positivity of Solution

**Theorem 1.** *Given the initial conditions of the state equations being nonnegative (thus $E(0) \geq 0$, $L(0) \geq 0$, $P(0) \geq 0$, $S_v(0) \geq 0$, $I_v(0) \geq 0$, $S_c(0) \geq 0$, $V_c(0) \geq 0$, $I_c(0) \geq 0$, $S_a(0) \geq 0$, $I_a(0) \geq 0$, $R_a(0) \geq 0$, and $V_a(0) \geq 0$), then the future solutions are also nonnegative (i.e., $E(t) \geq 0$, $L(t) \geq 0$, $P(t) \geq 0$, $S_v(t) \geq 0$, $I_v(t) \geq 0$, $S_c(t) \geq 0$, $V_c(t) \geq 0$, $I_c(t) \geq 0$, $S_a(t) \geq 0$, $I_a(t) \geq 0$, $R_a(t) \geq 0$, and $V_a(t) \geq 0$) for all $t > 0$.*

*Proof* 1. Given $t > 0$ as the initial time such that $E(t) = 0$. Then, from the first equation, we have $dE/dt = bN_v \geq 0$. Hence, $E(t) \geq 0\ \forall t > 0$.

Also, at a positive time $t$, if $S_v(t) = 0$, then the fourth equation becomes $S_v t = \Lambda_c + \rho_c I_c \geq 0$, which shows that $S_v(t) \geq 0$ and $\forall t > 0$. It is clear that the rest of the state variables can similarly be proven as nonnegative at any positive time. This concludes the proof. □

### 3.2. Boundedness and Feasible Region of Solutions of Model.

In this section, it is demonstrated that the model can be thoroughly examined within a specific area. We have provided the circumstances in the theorem below.

**Theorem 2.** *All solutions of Model (1) are uniformly bounded and contained in the feasible region defined by $\mathscr{D} = \mathscr{D}_v \times \mathscr{D}_h$, where $\mathscr{D}_v = \{(S_v(t), I_v(t)) \in \mathbb{R}_+^2 | N_v(t) \leq \Lambda_v/\mu_v\}$ and $\mathscr{D}_h = \{S_c(t), V_c(t), I_c(t), S_a(t), I_a(t), R_a(t), V_a(t) \in \mathbb{R}_+^7 | N_h(t) \leq \Lambda_c + \Lambda_a/\mu_h\}$. This implies that the region $\mathscr{D}$ is positively invariant under the flow defined by Model (1).*

*Proof* 2. If the total adult vector and human populations are identified by $N_v$ and $N_h$, then $N_v = S_v + I_v$ and $N_h = S_c + V_c + I_c + S_a + I_a + R_a + V_a$, respectively. Then, we have $N_v t = \Lambda_v - N_v\mu_v$ and $N_h t = \Lambda_c + \Lambda_a - N_h\mu_h - (\mu_{cm}I_c + \mu_{am}I_a)$.

From $N_v t$, we have $N_v t \leq \Lambda_v - N_v\mu_v$.

By standard comparison theorems [26], we have $N_v(t) \leq N_v(0)e^{-\mu_v t} + \Lambda_v/\mu_v(1 - e^{-\mu_v t})$ so that $\limsup_{t\longrightarrow\infty} N_v(t) \leq \Lambda_v/\mu_v$.

Also, from $N_v t$, we have $N_h(t) = N_h(0)e^{-\mu_h t} + \Lambda/\mu_h(1 - e^{-\mu_h t})$, where $\Lambda = \Lambda_c + \Lambda_a$.

Hence, all solutions are uniformly bounded.

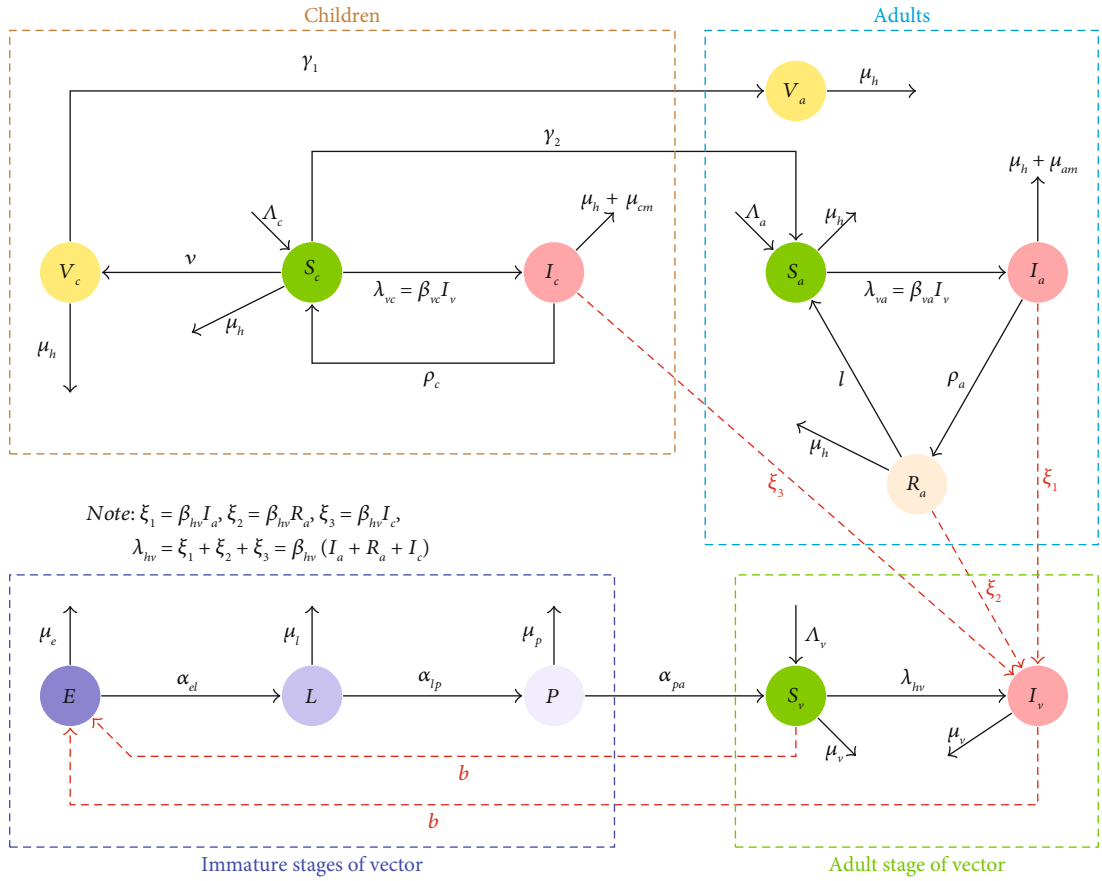


Figure 1: Compartmental diagram of the model.

Table 1: Description of parameters of the malaria model.

| Parameter | Description |
|---|---|
| $\nu$ | Vaccination rate among children |
| $\mu_h/\mu_v$ | Natural death rate in humans/vectors |
| $\mu_e$ | Failure rate of eggs to hatch |
| $\mu_l$ | Failure rate of larvae to develop into pupa |
| $\mu_p$ | Failure rate of pupae to develop into adult mosquitoes |
| $\alpha_{el}$ | Rate of transition from egg stage to larva stage |
| $\alpha_{lp}$ | Rate of transition from larva stage to pupa stage |
| $\alpha_{pa}$ | Rate of transition from pupa stage to susceptible mosquito |
| $\beta_{hv}$ | Probability of infection per contact with infected human |
| $\beta_{vc}(\beta_{va})$ | Probability of infection among children (adults) per contact with infectious mosquito |
| $b$ | Egg-laying rate in vectors |
| $\Lambda_c/\Lambda_a/\Lambda_v$ | Recruitment rate into children/adult/vector population |
| $\gamma_1(\gamma_2)$ | Transition rate of vaccinated (unvaccinated) children into adults |
| $\rho_c, (\rho_a)$ | Rate of recovery from malaria among children (adults) |
| $\mu_{cm}, (\mu_{am})$ | The mortality rate attributed to malaria in children (adults) |
| $\ell$ | Rate of waning of postmalaria recovery immunity in adults |
| $\xi_{1,2,3}$ | Rate of acquisition of protozoan from human reservoirs ($I_a$, $R_a$, and $I_c$, respectively) |

Let $\mathscr{D}_v = \{(S_v(t), I_v(t)) \in N_v(t) \le \Lambda_v/\mu_v\}$ and $\mathscr{D}_h = \{S_c(t), V_c(t), I_c(t), S_a(t), I_a(t), R_a(t), V_a(t) \in \mathbb{R}_+^7 | N_h(t) \le \Lambda/\mu_h\}$.

Then, the region $\mathscr{D} = \mathscr{D}_v \times \mathscr{D}_h$ is positively invariant under Model (1). Hence, the model is mathematically and epidemiologically well posed, and therefore, it is sufficient to study the model in $\mathscr{D}$. This concludes the proof. □

*3.3. Equilibrium Points.* The malaria-free equilibrium point is obtained when there are no infections, and hence, the forces of infections become zero (i.e., $\lambda_{vc}^* = \lambda_{va}^* = \lambda_{hv}^* = 0$) so that we obtain $\mathscr{E}^0 = (E^0, L^0, P^0, S_v^0, I_v^0, S_c^0, V_c^0, I_c^0, S_a, I_a^0, R_a^0, V_a^0)$, where

$$
\begin{aligned}
&\overbrace{E^0 = \frac{k_2k_3b\Lambda_v}{\mu_vk_3k_1k_2 - \alpha_{pa}\alpha_{lp}\alpha_{el}b},}^{\text{Immature Mosquitoes}}\\
&L^0 = \frac{k_3\alpha_{el}b\Lambda_v}{\mu_vk_3k_1k_2 - \alpha_{pa}\alpha_{lp}\alpha_{el}b},\\
&P^0 = \frac{\alpha_{lp}\alpha_{el}b\Lambda_v}{\mu_vk_3k_1k_2 - \alpha_{pa}\alpha_{lp}\alpha_{el}b};\\
&\overbrace{S_c^0 = \frac{\Lambda_c}{k_4},}^{\text{Children Population}}\\
&I_c^0 = 0,\\
&V_c^0 = \frac{\nu\Lambda_c}{k_4k_5};
\end{aligned}
\qquad
\begin{aligned}
&\overbrace{S_v^0 = \frac{k_1k_2k_3\Lambda_v}{\mu_vk_1k_2k_3 - \alpha_{pa}\alpha_{lp}\alpha_{el}b},}^{\text{Adult Vector Population}}\\
&I_v^0 = 0,\\
&\\
&\overbrace{S_a^0 = \frac{\Lambda_a}{\mu_h} + \frac{\gamma_2\Lambda_c}{\mu_hk_4},}^{\text{Adult Human Population}}\\
&I_a^0 = 0; R_a^0 = 0,\\
&V_a^0 = \frac{\nu\gamma_1\Lambda_c}{\mu_hk_5k_4}.
\end{aligned}
\tag{2}
$$

We then obtain the basic reproduction number by employing the technique described in [27, 28]. The $\mathscr{R}_0$ is taken as the largest eigenvalue (spectral radius) of the next-generation matrix $\mathscr{F}\mathscr{V}^{-1}$, given $F$ and $V$ are the transmission and transition matrices, respectively [27]. For our model, the infected subsystem consists of the $I_c$, $I_a$, $R_a$, and $I_v$ so that the matrices are given by

$$
\mathscr{V} = \begin{bmatrix} \mu_v & 0 & 0 & 0 \\ 0 & k_6 & 0 & 0 \\ 0 & 0 & k_7 & 0 \\ 0 & 0 & -\rho_a & k_8 \end{bmatrix} \quad \text{and}
$$

$$
\mathscr{F} = \begin{bmatrix} 0 & \beta_{hv}S_v^0 & \beta_{hv}S_v^0 & \beta_{hv}S_v^0 \\ \beta_{vc}S_c^0 & 0 & 0 & 0 \\ \beta_{va}S_a^0 & 0 & 0 & 0 \\ 0 & 0 & 0 & 0 \end{bmatrix}
$$

The basic reproduction number is thus given by

$$
\mathscr{R}_0 = \sqrt{\frac{\beta_{hv}S_v^0\left[\beta_{va}S_a^0k_6(k_8 + \rho_a) + \beta_{vc}S_c^0k_7k_8\right]}{k_6k_7k_8\mu_v}}
$$

The general endemic equilibrium point of Model (1) is given by $\mathscr{E}^* = (E^*, L^*, P^*, S_v^*, I_v^*, S_c^*, V_c^*, I_c^*, S_a, I_a^*, R_a^*, V_a^*)$, where

$$
\begin{aligned}
&\overbrace{E^* = \frac{k_2k_3b\Lambda_v}{\mu_vk_3k_1k_2 - \alpha_{pa}\alpha_{lp}\alpha_{el}b},}^{\text{Immature Mosquitoes}}\\
&L^* = \frac{k_3\alpha_{el}b\Lambda_v}{\mu_vk_3k_1k_2 - \alpha_{pa}\alpha_{lp}\alpha_{el}b},\\
&P^* = \frac{\alpha_{lp}\alpha_{el}b\Lambda_v}{\mu_vk_3k_1k_2 - \alpha_{pa}\alpha_{lp}\alpha_{el}b};\\
&\overbrace{S_c^* = \frac{k_6\Lambda_c}{(k_4k_6 + (k_6 - \rho_c)\lambda_{vc}^*)},}^{\text{Children Population}}\\
&I_c^* = \frac{\lambda_{vc}^*\Lambda_c}{(k_4k_6 + (k_6 - \rho_c)\lambda_{vc}^*)},\\
&V_c^* = \frac{k_6\nu\Lambda_c}{k_5(k_4k_6 + (k_6 - \rho_c)\lambda_{vc}^*)},
\end{aligned}
\qquad
\begin{aligned}
&\overbrace{S_v^* = \frac{\mu_v}{(\lambda_{hv}^* + \mu_v)}\left(\frac{k_1k_2k_3\Lambda_v}{\mu_vk_1k_2k_3 - \alpha_{pa}\alpha_{lp}\alpha_{el}b}\right),}^{\text{Adult Vector Population}}\\
&I_v^* = \frac{\lambda_{hv}^*}{(\lambda_{hv}^* + \mu_v)}\left(\frac{k_1k_2k_3\Lambda_v}{\mu_vk_1k_2k_3 - \alpha_{pa}\alpha_{lp}\alpha_{el}b}\right),\\
&\\
&\overbrace{S_a^* = \frac{k_7k_8(\Lambda_a + \gamma_2S_c)}{\mu_hk_7k_8 + (k_7k_8 - \rho_a\ell)\lambda_{va}^*},}^{\text{Adult Humans}}\\
&I_a^* = \frac{k_8(\Lambda_a + \gamma_2S_c)\lambda_{va}^*}{\mu_hk_7k_8 + (k_7k_8 - \rho_a\ell)\lambda_{va}^*},\\
&R_a^* = \frac{\rho_a\lambda_{va}^*(\Lambda_a + \gamma_2S_c)}{\mu_hk_7k_8 + (k_7k_8 - \rho_a\ell)\lambda_{va}^*},\\
&V_a^* = \frac{k_6\nu\gamma_1\Lambda_c}{\mu_hk_5(k_4k_6 + (k_6 - \rho_c)\lambda_{vc}^*)}.
\end{aligned}
\tag{3}
$$

where $\lambda_{va}^* = (\beta_{va}/\beta_{vc})\lambda_{vc}^*$ and $\lambda_{vc}^* = \beta_{vc}S_v^0\lambda_{hv}^*/(\lambda_{hv}^* + \mu_v)$, and $\lambda_{hv}^*$ satisfies the following polynomial equation:

$$
\Phi_2(\lambda_{hv}^*)^2 + \Phi_1\lambda_{hv}^* + \Phi_0 = 0
$$

$$
\Phi_2 = \left[k_4k_6 + (k_6 - \rho_c)\beta_{vc}S_v^0\right]\left[\mu_h\beta_{vc}k_7k_8 + (k_7k_8 - \rho_a\ell)\beta_{vc}\beta_{va}S_v^0\right]
$$

$$
\begin{aligned}
\Phi_1 = {} & \left[k_4k_6 + (\mu_h + \mu_{cm})\beta_{vc}S_v^0\right] \\
& \cdot \left[\mu_v\mu_h\beta_{vc}k_7k_8 - \beta_{hv}\beta_{vc}\beta_{va}S_v^0\Lambda_a(k_8 + \rho_a)\right] \\
& + \mu_v\mu_h\beta_{vc}k_7k_8k_4k_6 - \beta_{hv}\beta_{vc}\beta_{va}S_v^0k_6\gamma_2\Lambda_c(k_8 + \rho_a) \\
& - \mu_h\beta_{vc}k_7k_8\beta_{hv}\beta_{vc}S_v^0\Lambda_c + \mu_vk_4k_6\beta_{vc}\beta_{va}(k_7k_8 - \rho_a\ell)S_v^0 \\
& - \beta_{hv}\beta_{vc}\beta_{vc}\beta_{va}(k_7k_8 - \rho_a\ell)\left(S_v^0\right)^2\Lambda_c
\end{aligned}
$$

$$
\Phi_0 = \mu_v^2\mu_h\beta_{vc}k_7k_8k_4k_6\left(1 - \mathscr{R}^2\right)
\tag{4}
$$

The roots of Equation (4) are given by.

$$
\lambda_{hv}^* = \frac{-\Phi_1 \pm \sqrt{\Phi_1^2 - 4\Phi_2\Phi_0}}{2\Phi_2}
$$

Clearly, $\Phi_2 > 0$, and hence, the endemic equilibria of the model are characterized as follows:

1. The model has a unique endemic equilibrium whenever $\Phi_0 < 0$ (equivalently $\mathscr{R}_0 > 1$).

2. The model has two endemic equilibria whenever $\Phi_0 > 0$ (equivalently $\mathscr{R}_0 < 1$) and $\Phi_1 < 0$.

*3.4. Local Stability Analysis of Equilibrium Points.* Here, the indirect Lyapunov method is used to analyze the local stability of the malaria-free and malaria-persistent equilibrium points. With this approach, an equilibrium point $x^*$ of a model $xt = f(x)$ is considered as locally asymptotically stable if all eigenvalues of the Jacobian of the model evaluated at $x^*$ have negative real parts.

The Jacobian of Model (1) is given by

$$\mathscr{J} = \begin{bmatrix} \mathbb{J}_1 & \mathbb{J}_2 \\ \mathbb{J}_3 & \mathbb{J}_4 \end{bmatrix}$$

where $\mathbb{J}_1$, $\mathbb{J}_2$, $\mathbb{J}_3$, and $\mathbb{J}_4$ are defined in Appendix A.

The Jacobian $\mathscr{J}$, evaluated at $\mathscr{E}_{M0}$, has some of its eigenvalues as $-\mu_h$ (repeated twice), $-k_5$, and $-k_4$, and the rest satisfy the following characteristic polynomial equation:

$$\Psi_1(X)\Psi_2(X) = 0 \tag{5}$$

where

$$\Psi_1(X) = X^4 + \mathbb{A}_3X^3 + \mathbb{A}_2X^2 + \mathbb{A}_1X + \mathbb{A}_0$$

$$\Psi_2(X) = X^4 + \mathbb{B}_3X^3 + \mathbb{B}_2X^2 + \mathbb{B}_1X + \mathbb{B}_0$$

$$\mathbb{A}_3 = k_1 + k_2 + k_3 + \mu_v$$

$$\mathbb{A}_2 = (k_1 + k_2 + k_3)\mu_v + (k_2 + k_3)k_1 + k_2k_3$$

$$\mathbb{A}_1 = ((k_2 + k_3)k_1 + k_2k_3)\mu_v + k_2k_1k_3$$

$$\mathbb{A}_0 = k_3k_2k_1\mu_v - \alpha_{pa}\alpha_{lp}\alpha_{el}b$$

$$\mathbb{B}_3 = k_8 + k_7 + \mu_v + k_6$$

$$\mathbb{B}_2 = -\beta_{hv}S_v^0\left(\beta_{va}S_a^0 + S_c^0\beta_{vc}\right) + (k_6 + k_7 + k_8)\mu_v + (k_8 + k_7)k_6 + k_7k_8$$

$$\mathbb{B}_1 = -\beta_{hv}S_v^0\left[S_a^0(k_6 + k_8 + \rho_a)\beta_{va} + \beta_{vc}S_c^0(k_8 + k_7)\right] + ((k_8 + k_7)k_6 + k_7k_8)\mu_v + k_6k_7k_8$$

$$\mathbb{B}_0 = k_6k_7k_8\mu_v\left(1 - \mathscr{R}_0^2\right)$$

From Routh–Hurwitz stability conditions, the malaria-free equilibrium point is said to be locally asymptotically stable if the following conditions hold.

**Condition 1.** $\mathbb{A}_0 > 0, \mathbb{A}_3 > 0, \mathbb{A}_2 - \mathbb{A}_1/\mathbb{A}_3 > 0, \mathbb{A}_1 - \mathbb{A}_0\mathbb{A}_3/\mathbb{A}_2 - \mathbb{A}_1/\mathbb{A}_3 > 0$.

**Condition 2.** $\mathbb{B}_0 > 0, \mathbb{B}_3 > 0, \mathbb{B}_2 - \mathbb{B}_1/\mathbb{B}_3 > 0, \mathbb{B}_1 - \mathbb{B}_0\mathbb{B}_3/\mathbb{B}_2 - \mathbb{B}_1/\mathbb{B}_3 > 0$.

Substituting the expressions for $\mathbb{A}_i$, $i = 1, 2, 3$ and simplifying shows that Condition (1) holds always. Condition (2) holds only when $\mathscr{R}_0 < 1$. The following result is therefore established.

**Theorem 3.** *The disease-free equilibrium point $\mathscr{E}_{M0}$ is locally asymptotically stable whenever $\mathscr{R}_0 < 1$ and unstable otherwise.*

*3.5. Global Stability of the Malaria-Free Equilibrium Point.* To study the global stability of the malaria-free equilibrium point, we adopt the direct Lyapunov technique by defining the Lyapunov function candidate given by

$$\mathscr{L} = \mathscr{K}_1I_c + \mathscr{K}_2I_a + \mathscr{K}_3R_a + \mathscr{K}_4I_v$$

where

$$\mathscr{K}_1 = \beta_{vh}\left[\left(S_a^0(k_8 + \rho_a)k_6 + k_8S_c^0k_7\right)\beta_{hv} + k_6k_7k_8\right],$$

$$\mathscr{K}_2 = \beta_{hv}k_7k_8\left(S_v^0\beta_{vh} + \mu_v\right)$$

$$\mathscr{K}_3 = \beta_{hv}k_6\left(S_v^0\beta_{vh} + \mu_v\right)(k_8 + \rho_a),$$

$$\mathscr{K}_4 = k_6\beta_{hv}k_7\left(S_v^0\beta_{vh} + \mu_v\right)$$

The time derivative of the Lyapunov function is then given by

$$\mathscr{L}t = \mathscr{K}_1I_ct + \mathscr{K}_2I_at + \mathscr{K}_3R_at + \mathscr{K}_4I_vt$$

Substituting the appropriate equations into the time-derivative of $\mathscr{L}$ and simplifying gives

$$\mathscr{L}t = \frac{\beta_{hv}\beta_{vh}}{\mathscr{R}_0^2}\left[\left(S_a^0(k_8 + \rho_a)k_6 + k_8S_c^0k_7\right)\left(\mathscr{R}_0^2S_v - S_v^0\right)\beta_{hv} + \mathscr{R}_0^2k_6k_7k_8\left(S_v - S_v^0\right)\right](I_a + I_c + R_a) + [xx]I_v$$

*3.6. Sensitivity Analysis of $\mathscr{R}_0$.* Sensitivity analysis helps understand how small adjustments in parameter values impact disease transmission. In this study, the sensitivity of malaria transmission to parameter changes was assessed using the basic reproduction number $\mathscr{R}_0$, which indicates whether the disease might be eliminated or persist. The analysis utilized the normalized forward sensitivity index.

If $\mathscr{R}_0$ is a differentiable function $P$, then the normalized forward sensitivity index of $\mathscr{R}_0$ relative to $P$ is stated as

$$\mathscr{A}_p^{\mathscr{R}_0} = \frac{\partial\mathscr{R}_0}{\partial p} \times \frac{p}{\mathscr{R}_0}$$

The sensitivity indexes are given as follows:

$$\mathscr{A}^{\mathscr{R}_0}_{\alpha_{el}} = \frac{\alpha_{lp}\alpha_{pa}\mu_e\alpha_{el}}{2\left(\mu_v k_1 k_2 k_3 - \alpha_{el}\alpha_{lp}\alpha_{pa}\right)k_1},$$

$$\mathscr{A}^{\mathscr{R}_0}_{\alpha_{pa}} = \frac{\alpha_{el}\alpha_{lp}\mu_p\alpha_{pa}}{2\left(\mu_v k_1 k_2 k_3 - \alpha_{el}\alpha_{lp}\alpha_{pa}\right)k_3}$$

$$\mathscr{A}^{\mathscr{R}_0}_{\beta_{va}} = \frac{k_5(k_8+\rho_a)\beta_{va}(k_4\Lambda_a+\gamma_2\Lambda_c)k_6}{2\hbar_1}$$

$$\mathscr{A}^{\mathscr{R}_0}_{\Lambda_v} = \frac{1}{2}$$

$$\mathscr{A}^{\mathscr{R}_0}_{\Lambda_a} = \frac{k_4k_5k_6(k_8+\rho_a)\beta_{va}\Lambda_a}{2\hbar_1},$$

$$\mathscr{A}^{\mathscr{R}_0}_{\mu_l} = \frac{\alpha_{el}\alpha_{pa}\mu_l\alpha_{lp}}{2\left(\alpha_{el}\alpha_{lp}\alpha_{pa} - \mu_v k_1 k_2 k_3\right)k_2},$$

$$\mathscr{A}^{\mathscr{R}_0}_{\mu_v} = \frac{-2\mu_v k_1 k_2 k_3 + \alpha_{el}\alpha_{lp}\alpha_{pa}}{2\left(\mu_v k_1 k_2 k_3 - \alpha_{el}\alpha_{lp}\alpha_{pa}\right)}$$

$$\mathscr{A}^{\mathscr{R}_0}_{\mu_{am}} = -\frac{(k_4\Lambda_a+\gamma_2\Lambda_c)k_5\mu_{am}\beta_{va}(k_8+\rho_a)k_6}{2\hbar_1k_7},$$

$$\mathscr{A}^{\mathscr{R}_0}_{\gamma_1} = -\frac{\mu_h k_7 k_8\beta_{vc}\Lambda_c\gamma_1\nu}{2k_5\hbar_1},$$

$$\mathscr{A}^{\mathscr{R}_0}_{\rho_c} = -\frac{\rho_c\nu\Lambda_c\beta_{vc}k_8k_7\mu_h}{2\hbar_1k_6},$$

$$\mathscr{A}^{\mathscr{R}_0}_{\ell} = -\frac{k_5\ell\beta_{va}\rho_a(k_4\Lambda_a+\gamma_2\Lambda_c)k_6}{2k_8\hbar_1}$$

$$\mathscr{A}^{\mathscr{R}_0}_{\alpha_{lp}} = \frac{\alpha_{el}\alpha_{pa}\mu_l\alpha_{lp}}{2\left(\mu_v k_1 k_2 k_3 - \alpha_{el}\alpha_{lp}\alpha_{pa}\right)k_2}$$

$$\mathscr{A}^{\mathscr{R}_0}_{\beta_{hv}} = \frac{1}{2}$$

$$\mathscr{A}^{\mathscr{R}_0}_{\beta_{vc}} = \frac{\nu\beta_{vc}\Lambda_c k_7 k_8\mu_h}{2\hbar_1}$$

$$\mathscr{A}^{\mathscr{R}_0}_{\Lambda_c} = \frac{\Lambda_c(\gamma_2k_6(k_8+\rho_a)\beta_{va}k_5 + \beta_{vc}\nu k_7k_8\mu_h)}{2\hbar_1}$$

$$\mathscr{A}^{\mathscr{R}_0}_{\mu_e} = \frac{\alpha_{lp}\alpha_{pa}\mu_e\alpha_{el}}{2\left(\alpha_{el}\alpha_{lp}\alpha_{pa} - \mu_v k_1 k_2 k_3\right)k_1}$$

$$\mathscr{A}^{\mathscr{R}_0}_{\mu_p} = \frac{\alpha_{el}\alpha_{lp}\mu_p\alpha_{pa}}{2\left(\alpha_{el}\alpha_{lp}\alpha_{pa} - \mu_v k_1 k_2 k_3\right)k_3}$$

$$\mathscr{A}^{\mathscr{R}_0}_{\mu_{cm}} = -\frac{\mu_{cm}\nu\Lambda_c\beta_{vc}k_8k_7\mu_h}{2\hbar_1k_6}$$

$$\mathscr{A}^{\mathscr{R}_0}_{\nu} = -\frac{\nu\mu_h\Lambda_c\beta_{vc}k_8k_7 + \nu\Lambda_c\beta_{va}\gamma_2(\ell+\mu_h+\rho_a)k_6}{2\hbar_2k_4}$$

$$\mathscr{A}^{\mathscr{R}_0}_{\gamma_2} = \frac{\gamma_2\Lambda_c((\mu_h+\nu)k_6(k_8+\rho_a)\beta_{va}k_5 - \beta_{vc}\nu k_7k_8\mu_h)}{2\hbar_1k_4}$$

$$\mathscr{A}^{\mathscr{R}_0}_{\rho_a} = -\frac{(k_4\Lambda_a+\gamma_2\Lambda_c)k_5\rho_a\beta_{va}k_6(\ell-\mu_{am})}{2\hbar_1k_7}$$

with $\hbar_1 = k_5k_6\beta_{va}(k_8+\rho_a)(k_4\Lambda_a+\gamma_2\Lambda_c) + \beta_{vc}\Lambda_c\nu k_7k_8\mu_h$,

$\hbar_2 = \Lambda_c\beta_{vc}k_8k_7\mu_h + \beta_{va}k_6(k_8+\rho_a)(k_4+\gamma_2\Lambda_c)$

Table 2: Sensitivity indices of $\mathscr{R}_0$ with respect to model parameters.

| Parameter | Numerical sensitivity index | Parameter | Numerical sensitivity index |
|---|---|---|---|
| $\alpha_{el}$ | −0.2222 | $\mu_p$ | 0.2500 |
| $\alpha_{lp}$ | −0.2857 | $\mu_h$ | −0.9201 |
| $\alpha_{pa}$ | −0.2500 | $\mu_{cm}$ | −0.0099 |
| $\beta_{hv}$ | 0.5000 | $\mu_{am}$ | −0.0635 |
| $\beta_{va}$ | 0.4316 | $\mu_v$ | −0.3334 |
| $\beta_{vc}$ | 0.0684 | $\nu$ | $-4.1759\times10^{-4}$ |
| $\Lambda_v$ | 1/2 | $\gamma_2$ | $8.9708\times10^{-5}$ |
| $\Lambda_c$ | 0.0685 | $\rho_a$ | $3.6437\times10^{-06}$ |
| $\Lambda_a$ | 0.4315 | $\rho_c$ | −0.0062 |
| $\mu_e$ | 0.2222 | $b$ | −0.6666 |
| $\mu_l$ | 0.2857 | $l$ | $-2.4706\times10^{-7}$ |

Table 3: Parameter values used for simulations.

| Parameter | Value per day | Source |
|---|---|---|
| $\nu$ | 0.01 | Assumed |
| $\mu_h$ | 1.6300 | [29] |
| $\mu_v$ | 0.119 | Assumed |
| $\mu_e$ | 0.3 | [24] |
| $\mu_l$ | 0.3 | [24] |
| $\mu_p$ | 0.15 | [24] |
| $\alpha_{el}$ | 0.60 | [24] |
| $\alpha_{lp}$ | 0.40 | [24] |
| $\alpha_{pa}$ | 0.25 | [24] |
| $\Lambda_v$ | 5.000 | Assumed |
| $b$ | 2.0 | [24] |
| $\Lambda_c$ | 10 | Assumed |
| $\Lambda_a$ | 20 | Assumed |
| $\gamma_1$ | 0.10 | [29] |
| $\gamma_2$ | 0.001 | [29] |
| $\rho_c$ | 0.1930 | Assumed |
| $\rho_a$ | 0.0001 | Assumed |
| $\mu_{cm}$ | 0.3100 | [29] |
| $\mu_{am}$ | 0.2810 | [29] |
| $\ell$ | 0.0155 | Assumes |
| $\beta_{hv}$ | 0.0452 | Assumed |
| $\beta_{va}$ | 0.0320 | Assumed |
| $\beta_{vc}$ | 0.0114 | Assumed |

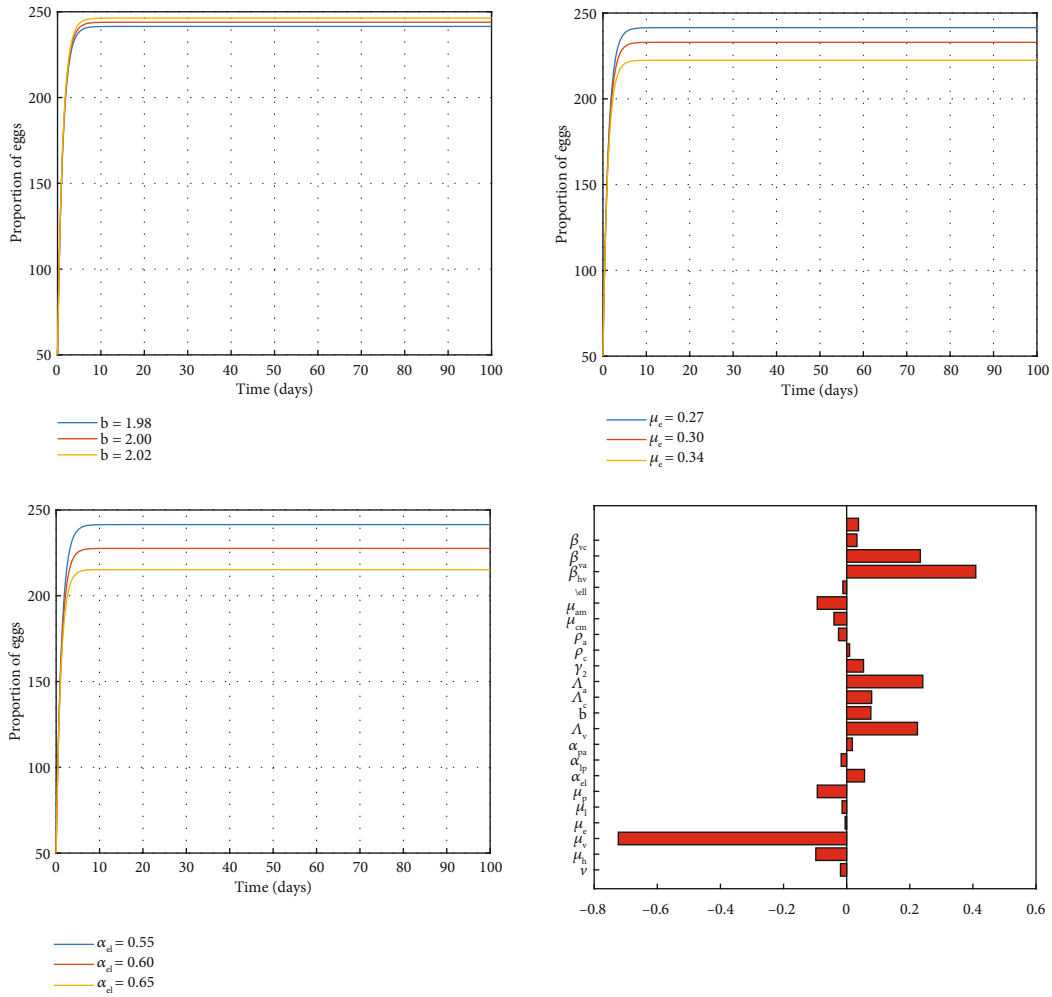


Figure 2: A time graph showing the impact of $b$, $\mu_e$, and $\alpha_{el}$ on the egg class and sensitivity plot.

The sensitivity indices for $\mathcal{R}_0$ concerning the model parameters are computed and detailed in Table 2, utilizing the parameter values specified in Table 3. These sensitivity indices illustrate the percentage alteration in a model's output due to a percentage shift in the model parameter. A positive (negative) sensitivity index of a parameter signifies that a percentage rise (decline) in the model parameter leads to an increase (decrease) in $\mathcal{R}_0$. Conversely, a negative 100 sensitivity index suggests that an increase (decrease) in the parameter's value will induce a decrease (increase) in $\mathcal{R}_0$. The corresponding Latin hypercube plot is represented in Figure 2.

*3.7. Bifurcation Analysis.* The center manifold theory as described in Theorem 4.1 of [30] is used for the bifurcation analysis.

Using this method, we choose $\beta_{hv} = \beta^*_{hv} = k_6k_7k_8\mu_v/S^0_v(\beta_{va}S^0_ak_6k_8 + \beta_{va}S^0_ak_6\rho_a + \beta_{vc}S^0_ck_7k_8)$ as a bifurcation parameter in which case the Jacobian of the model at $\mathcal{E}_{M0}$ will have a zero simple eigenvalue. The right and left eigenvectors associated with this zero eigenvalue are given by

$$\mathbf{w} = \left(0, 0, 0, -w_5, w_5, -\frac{S_cw_5(k_6-\rho_c)\beta_{vc}}{k_6k_4}, -\frac{\nu S_cw_5(k_6-\rho_c)\beta_{vc}}{k_6k_4k_5}, \frac{\beta_{vc}S_cw_5}{k_6}, w_9, \frac{\beta_{va}S_aw_5}{k_7}, \frac{\beta_{va}S_a\rho_aw_5}{k_7k_8}, w_{12}\right)^T$$

$$\mathbf{v} = \left(0, 0, 0, 0, \nu_5, 0, 0, \frac{\beta_{hv}S_v\nu_5}{k_6}, 0, \frac{\beta_{hv}S_v(k_8+\rho_a)\nu_5}{k_7k_8}, \frac{\beta_{hv}S_v\nu_5}{k_8}, 0\right), \text{where}$$

$$w_9 = \left(\frac{\beta_{va}S_a(\ell\rho_a - k_7k_8)}{k_7k_8\mu_h} - \frac{\gamma_2S_c(k_6-\rho_c)\beta_{vc}}{k_6k_4\mu_h}\right)w_5 \quad \text{and} \quad w_{12} = -\frac{\gamma_1\nu S_cw_5(k_6-\rho_c)\beta_{vc}}{k_6k_4\mu_hk_5}$$

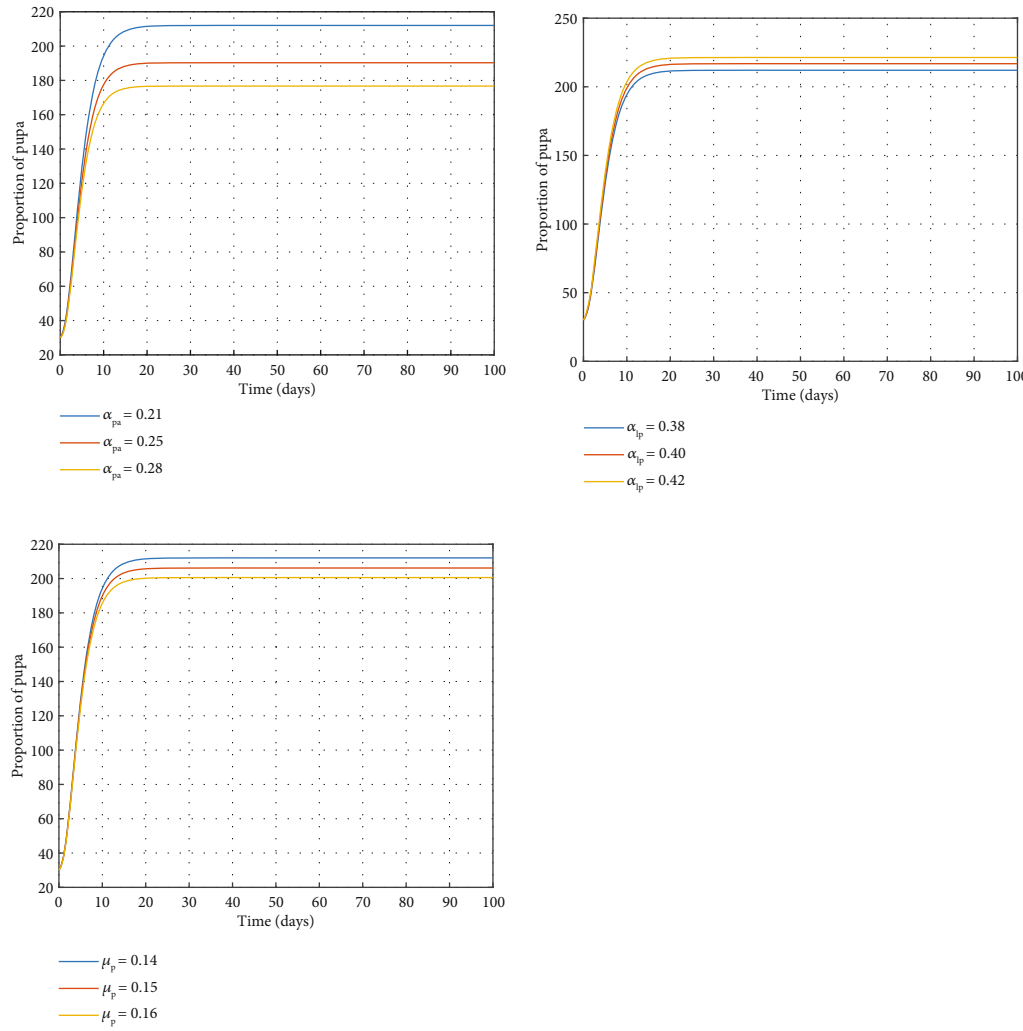


FIGURE 3: A time graph depicting the impact of $\alpha_{pa}$, $\alpha_{lp}$, and $\mu_p$ on the pupa class.

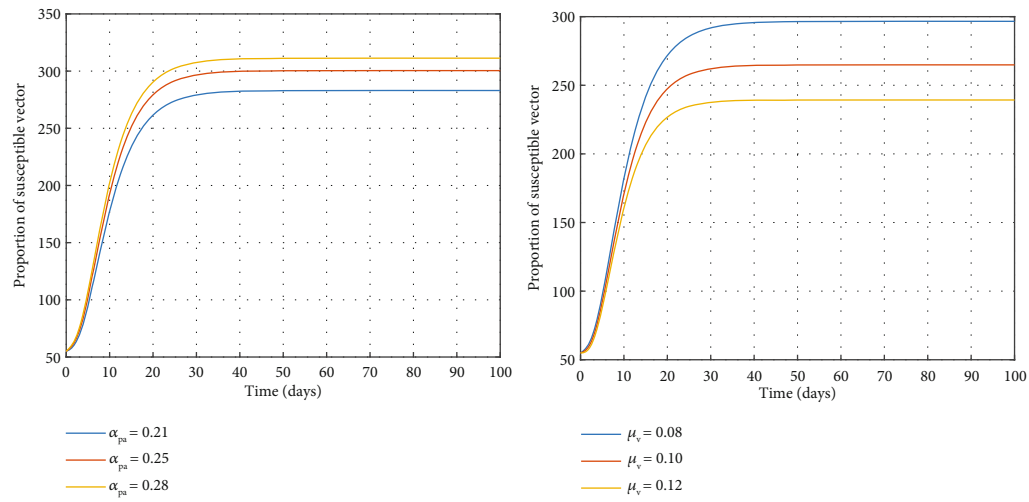


FIGURE 4: A time graph depicting the impact of $\alpha_{pa}$ and $\mu_v$ on the susceptible vector class.

The bifurcation coefficients are thus given by

$$\mathbf{a} = -2\beta_{hv}^{*}\left[\frac{S_a^0\beta_{va}(k_8+\rho_a)}{k_7k_8} + \frac{S_c^0\beta_{vc}}{k_6} + \frac{\beta_{vc}^2S_c^0(k_6-\rho_c)S_v^0}{k_6^2k_4} + \left(\frac{\beta_{va}S_a^0(k_7k_8-\ell\rho_a)}{k_7^2k_8^2\mu_h} + \frac{\gamma_2S_c^0\beta_{vc}(k_6-\rho_c)}{k_6k_4\mu_hk_7k_8}\right)S_v^0(k_8+\rho_a)\beta_{va}\right]\nu_5\omega_5^2$$

$$\mathbf{b} = \frac{S_v^0\left(S_a^0\beta_{va}(k_8+\rho_a)k_6 + S_c^0\beta_{vc}k_7k_8\right)\nu_5\omega_5}{k_7k_8k_6}$$

Clearly, $\mathbf{a} < 0$ and $\mathbf{b} > 0$, and hence following Theorem 4.1 of [30], the following result is established.

**Theorem 4.** *Bifurcation at $\mathscr{R}_0 = 1$.*

1. *Whenever $\mathscr{R}_0 < 1$, then the malaria-free equilibrium is locally asymptotically stable, and there is no endemic equilibrium.*
2. *Whenever $\mathscr{R}_0 > 1$, then the malaria-free equilibrium is unstable, and a stable endemic equilibrium appears.*
3. *The Malaria Model (1) exhibits forward bifurcation at $\mathscr{R}_0 = 1$.*

## 4. Numerical Simulation

In this section, we carried out numerical simulations to illustrate some analytical conclusions and to analyze the impact of some model parameters on the dynamics of malaria. MATLAB software with the Runge–Kutta fourth-order method was used in the numerical simulation for the model of Equation (1). The values of the parameters are given in Table 3 and the initial conditions $E(0) = 50$, $L(0) = 40$, $P(0) = 30$, $S_v(0) = 55$, $I_v(0) = 45$, $S_c(0) = 50$, $S_a(0) = 200$, $I_c(0) = 500$, $I_a(0) = 350$, $V_c(0) = 30$, $R_a(0) = 400$, and $V_a(0) = 20$.

From Figure 2, the rate of growth of egg numbers is proportional to the egg-laying rate in vectors ($b$). An increase or decrease in the growth of eggs results in a corresponding change of $b$. This therefore increases the population of the larva (L) class. Failure rate of eggs to hatch ($\mu_e$) and rate of transfer from egg stage to larva stage ($\alpha_{el}$) are inversely proportional to the rate of growth of the egg population. That is, an increase in $\mu_e$ or $\alpha_{el}$ leads to a decrease in the population of the egg compartment and consequently a decrease in the larva population.

Figure 3 shows a negative correlation between the rate of transfer from the pupa stage to susceptible mosquitoes ($\alpha_{pa}$) and the pupal population. It means an increase in one quantity leads to a decrease in another and subsequently a decrease in the population of the next compartment, that is, the susceptible mosquitoes. When the rate of transfer from larva stage to the pupa stage ($\alpha_{lp}$) increases, it results in a corresponding increment in the population of the pupal class and vice versa. This obviously will result in an increase in the larval population. The graph also indicates an indirect proportion between the parameter and the variable. For this reason, an increase in the failure rate of pupae to develop into adult mosquitoes ($\mu_p$) will yield a reduction in the number of pupa.

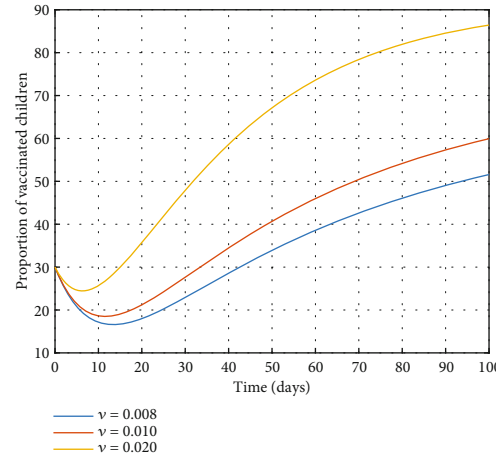


FIGURE 5: A time graph depicting the impact of $\nu$ on the vaccinated children class.

A decrease in the rate of transfer from the pupa stage to susceptible mosquitoes ($\alpha_{pa}$) always results in a corresponding decrease in the population of susceptible vectors and vice versa, as seen in Figure 4. An increase in the natural death rate in adult vectors ($\mu_v$) will lead to a decrease in the susceptible vector population and eventually a decline in the population of the infected vector compartment.

Increasing or decreasing the vaccination rate among children ($\nu$) results in an initial fall in the number of vaccinated children as displayed in Figure 5. But then, after some days, there is a great increment in the vaccinated children population. It is clear that increasing $\nu$ will result in the growth of the proportion of vaccinated children.

## 5. Conclusions

In this research, we proposed a mathematical model to study the impact of immature mosquitoes and vaccination on the transmission dynamics of malaria. The basic reproduction number is computed to measure the potential of the disease. The disease-free and endemic equilibrium points are shown to be asymptotically stable whenever $\mathscr{R}_0 \leq 1$ and $\mathscr{R}_0 > 1$, respectively. The sensitivity analysis and numerical simulations performed confirmed that parameters with positive sensitivity indices should be decreased, while the parameters that are inversely related to the basic reproduction number should be increased so as to minimise the transmission of malaria. The analysis further showed that in the management of malaria, immature mosquitoes are essential. It therefore suggests that individuals, the general public, and the government must strengthen activities and campaigns and formulate policies to control the immature stages of the vector at all levels (homes, markets, institutions, and firms) to eradicate malaria completely. These findings are supported by [16].

The use of vaccines in newborn babies also helps in mitigating malaria, as shown in the analysis.

## Appendix A

$$\mathbb{J}_1 = \begin{bmatrix} -k_1 & 0 & 0 & b & b & 0 \\ \alpha_{el} & -k_2 & 0 & 0 & 0 & 0 \\ 0 & \alpha_{lp} & -k_3 & 0 & 0 & 0 \\ 0 & 0 & \alpha_{pa} & -\lambda_{hv} - \mu_v & 0 & 0 \\ 0 & 0 & 0 & \lambda_{hv} & -\mu_v & 0 \\ 0 & 0 & 0 & 0 & -\beta_{vc} S_c & -\beta_{vc} I_v - k_4 \end{bmatrix}, \quad \mathbb{J}_2 = \begin{bmatrix} 0 & 0 & 0 & 0 & 0 & 0 \\ 0 & 0 & 0 & 0 & 0 & 0 \\ 0 & 0 & 0 & 0 & 0 & 0 \\ 0 & -\beta_{hv} S_v & 0 & -\beta_{hv} S_v & -\beta_{hv} S_v & 0 \\ 0 & \beta_{hv} S_v & 0 & \beta_{hv} S_v & \beta_{hv} S_v & 0 \\ 0 & \rho_c & 0 & 0 & 0 & 0 \end{bmatrix}$$

$$\mathbb{J}_3 = \begin{bmatrix} 0 & 0 & 0 & 0 & 0 & \nu \\ 0 & 0 & 0 & 0 & \beta_{vc} S_c & \beta_{vc} I_v \\ 0 & 0 & 0 & 0 & -\beta_{va} S_a & \gamma_2 \\ 0 & 0 & 0 & 0 & \beta_{va} S_a & 0 \\ 0 & 0 & 0 & 0 & 0 & 0 \\ 0 & 0 & 0 & 0 & 0 & 0 \end{bmatrix}, \quad \mathbb{J}_4 = \begin{bmatrix} 0 & 0 & 0 & 0 & 0 & \nu \\ 0 & 0 & 0 & 0 & \beta_{vc} S_c & \beta_{vc} I_v \\ 0 & 0 & 0 & 0 & -\beta_{va} S_a & \gamma_2 \\ 0 & 0 & 0 & 0 & \beta_{va} S_a & 0 \\ 0 & 0 & 0 & 0 & 0 & 0 \\ 0 & 0 & 0 & 0 & 0 & 0 \end{bmatrix} \tag{A.1}$$

## Data Availability Statement

All data used to support the findings of this study are included within the article.

## Conflicts of Interest

The authors declare no conflicts of interest.

## Funding

There is no funding from any institution or organization.

## References

[1] L. S. Garcia, "Malaria update for the clinical microbiology laboratory: a new species, Plasmodium knowlesi, and new diagnostic tests," *Clinical Microbiology Newsletter*, vol. 32, no. 17, pp. 127–133, 2010.

[2] W H Organization, "Malaria," 2022, August 2022, https://www.who.int/health-topics/malaria.

[3] H. W. Hethcote, "The mathematics of infectious diseases," *SIAM Review*, vol. 42, no. 4, pp. 599–653, 2000.

[4] R. Aggarwal and Y. A. Raj, "A fractional order HIV-TB co-infection model in the presence of exogenous reinfection and recurrent TB," *Nonlinear Dynamics*, vol. 104, no. 4, pp. 4701–4725, 2021.

[5] R. Tanvi and R. Aggarwal, "Estimating the impact of antiretroviral therapy on HIV-TB co-infection: optimal strategy prediction," *International Journal of Biomathematics*, vol. 14, no. 1, article 2150004, 2021.

[6] Tanvi and R. Aggarwal, "Stability analysis of a delayed HIV-TB co-infection model in resource limitation settings," *Chaos, Solitons & Fractals*, vol. 140, article 110138, 2020.

[7] R. Tanvi, R. Aggarwal, and T. Kovacs, "Assessing the effects of Holling type-II treatment rate on HIV-TB Co-infection," *Acta Biotheoretica*, vol. 69, no. 1, pp. 1–35, 2021.

[8] S. Opoku, B. Seidu, and P. N. Akuka, "A mathematical analysis of the impact of maternally derived immunity and double-dose vaccination on the spread and control of measles," *Computational and Mathematical Biophysics*, vol. 11, no. 1, p. 20230106, 2023.

[9] P. N. Akuka, B. Seidu, and C. S. Bornaa, "Mathematical analysis of COVID-19 transmission dynamics model in Ghana with double-dose vaccination and quarantine," *Computational and Mathematical Methods in Medicine*, vol. 2022, Article ID 7493087, 10 pages, 2022.

[10] A. Apam, B. Seidu, and C. Bornaa, "A mathematical model of the spread and control of novel coronavirus disease with post-recovery symptoms," *Asia Pacific Journal of Mathematics*, vol. 9, p. 5, 2022.

[11] C. J. Whitty and E. Ansah, "Malaria control stalls in high incidence areas," *BMJ*, vol. 365, article l2216, 2019.

[12] S. I. Oke, M. M. Ojo, M. O. Adeniyi, and M. B. Matadi, "Mathematical modeling of malaria disease with control strategy," *Communications in Mathematical Biology and Neuroscience*, vol. 2020, p. 43, 2020.

[13] A. I. Abioye, M. O. Ibrahim, O. J. Peter, and H. A. Ogunseye, "Optimal control on a mathematical model of malaria," *Scientific Bulletin-Series A: Applied Mathematics and Physics*, vol. 82, no. 3, pp. 178–190, 2020.

[14] E. A. Iboi, A. B. Gumel, and J. E. Taylor, "Mathematical modeling of the impact of periodic release of sterile male mosquitoes

and seasonality on the population abundance of malaria mosquitoes," *Journal of Biological Systems*, vol. 28, no. 2, pp. 277–310, 2020.

[15] P. Layie, V. C. Kamla, J. C. Kamgang, and Y. E. Wono, "Agent-based modeling of malaria control through mosquito aquatic habitats management in a traditional sub-Sahara grouping," *BMC Public Health*, vol. 21, no. 1, p. 487, 2021.

[16] O. Koutou, B. Traoré, and B. Sangaré, "Mathematical modeling of malaria transmission global dynamics: taking into account the immature stages of the vectors," *Advances in Difference Equations*, vol. 2018, no. 1, 2018.

[17] B. Traoré, O. Koutou, and B. Sangaré, "A global mathematical model of malaria transmission dynamics with structured mosquito population and temperature variations," *Nonlinear Analysis: Real World Applications*, vol. 53, p. 103081, 2020.

[18] S. Olaniyi, M. Mukamuri, K. O. Okosun, and O. A. Adepoju, "Mathematical analysis of a social hierarchy-structured model for malaria transmission dynamics," *Results in Physics*, vol. 34, article 104991, 2022.

[19] S. Tchoumi, E. Z. Dongmo, J. C. Kamgang, and J. M. Tchuenche, "Dynamics of a two-group structured malaria transmission model," *Informatics in Medicine Unlocked*, vol. 29, article 100897, 2022.

[20] L. M. Beck-Johnson, W. A. Nelson, K. P. Paaijmans, A. F. Read, M. B. Thomas, and O. N. Bjørnstad, "The effect of temperature on Anopheles mosquito population dynamics and the potential for malaria transmission," *PLoS One*, vol. 8, no. 11, article e79276, 2013.

[21] J. Lu and J. Li, "Dynamics of stage-structured discrete mosquito population models," *Journal of Applied Analysis & Computation*, vol. 1, no. 1, pp. 53–67, 2011.

[22] X. Wang and X.-Q. Zhao, "A climate-based malaria model with the use of bed nets," *Journal of Mathematical Biology*, vol. 77, no. 1, pp. 1–25, 2018.

[23] D. Moulay, M. A. Aziz-Alaoui, and M. Cadivel, "The chikungunya disease: modeling, vector and transmission global dynamics," *Mathematical Biosciences*, vol. 229, no. 1, pp. 50–63, 2011.

[24] A. Abdelrazec and A. B. Gumel, "Mathematical assessment of the role of temperature and rainfall on mosquito population dynamics," *Journal of Mathematical Biology*, vol. 74, no. 6, pp. 1351–1395, 2017.

[25] A. M. Lutambi, M. A. Penny, T. Smith, and N. Chitnis, "Mathematical modelling of mosquito dispersal in a heterogeneous environment," *Mathematical Biosciences*, vol. 241, no. 2, pp. 198–216, 2013.

[26] V. Lakshmikantham, S. Leela, and A. A. Martynyuk, *Stability Analysis of Nonlinear Systems*, Springer, 1990.

[27] O. Diekmann, J. A. P. Heesterbeek, and J. A. J. Metz, "On the definition and the computation of the basic reproduction ratio R 0 in models for infectious diseases in heterogeneous populations," *Journal of Mathematical Biology*, vol. 28, no. 4, pp. 365–382, 1990.

[28] J. K. K. Asamoah, B. Safianu, E. Afrifa et al., "Optimal control dynamics of gonorrhea in a structured population," *Heliyon*, vol. 9, no. 10, article e20531, 2023.

[29] A. Ducrot, S. B. Sirima, B. Somé, and P. Zongo, "A mathematical model for malaria involving differential susceptibility, exposedness and infectivity of human host," *Journal of Biological Dynamics*, vol. 3, no. 6, pp. 574–598, 2009.

[30] C. Castillo-Chavez and B. Song, "Dynamical models of tuberculosis and their applications," *Mathematical Biosciences & Engineering*, vol. 1, no. 2, pp. 361–404, 2004.